

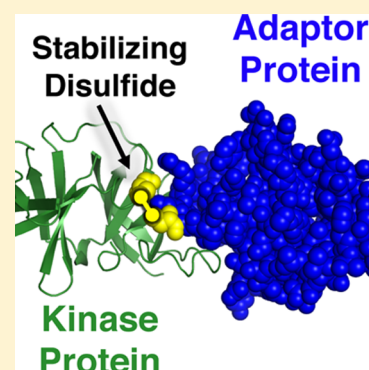


# Increasing and Decreasing the Ultrastability of Bacterial Chemotaxis Core Signaling Complexes by Modifying Protein–Protein Contacts

Kene N. Piasta and Joseph J. Falke\*

Department of Chemistry and Biochemistry and Molecular Biophysics Program, University of Colorado, Boulder, Colorado 80309-0596, United States

**ABSTRACT:** The chemosensory signaling array of bacterial chemotaxis is composed of functional core units containing two receptor trimers of dimers, a homodimeric CheA kinase, and two CheW adaptor proteins. *In vitro* reconstitutions generate individual, functional core units and larger functional assemblies, including dimers, hexagons, and hexagonal arrays. Such reconstituted complexes have been shown to have both quasi-stable and ultrastable populations that decay with lifetimes of 1–2 days and ~3 weeks at 22 °C, respectively, where decay results primarily from proteolysis of the bound kinase [Erbse, A. H., and Falke, J. J. (2009) *Biochemistry* 48, 6975–6987; Slivka, P. F., and Falke, J. J. (2012) *Biochemistry* 51, 10218–10228]. In this work, we show that the ultrastable population can be destabilized to the quasi-stable level via the introduction of a bulky tryptophan residue at either one of two essential protein–protein interfaces within the core unit: the receptor–kinase contact or kinase–adaptor interface 1. Moreover, we demonstrate that the quasi-stable population can be made ultrastable via the introduction of a disulfide bond that covalently stabilizes the latter interface. The resulting disulfide at least doubles the functional lifetime of the ultrastable population, to  $\geq 5.9$  weeks at 22 °C, by protecting the kinase from endogenous and exogenous proteases. Together, these results indicate that the ultrastability of reconstituted core complexes requires well-formed contacts among the receptor, kinase, and adaptor proteins, whereas quasi-stability arises from less perfect contacts that allow slow proteolysis of the bound kinase. Furthermore, the results reveal that ultrastability, and perhaps the size or order of chemosensory complexes and arrays, can be increased by an engineered disulfide bond that covalently cross-links a key interface. Overall, it appears that native ultrastability has evolved to provide an optimal rather than maximal level of kinetic durability, suggesting that altered selective pressure could either increase or decrease the functional lifetime of core complexes.



Motile bacterial and archaeal cells possess a conserved chemosensory pathway that senses external chemical gradients and controls cell movement, allowing migration toward an optimal living environment (reviewed in refs 3–10). This chemotactic behavior plays a crucial role in cell survival under nutrient limiting conditions, as well as in pathogenic wound or tissue seeking during infection.<sup>11–13</sup>

The protein components of the chemosensory pathway include receptors, kinases, phosphatases, adaptor proteins, and adaptation proteins, all of which assemble to form a membrane-bound, hexagonal-lattice array.<sup>5,10,14–27</sup> The core structural proteins of this chemosensory array are the transmembrane receptor, histidine kinase CheA, and adaptor protein CheW. Together, these three proteins form a core unit composed of (i) two receptor oligomers, each a trimer of homodimers, (ii) one kinase homodimer, and (iii) two adaptor molecules.<sup>17,18,21,22,26–30</sup> Three of these core units join to form a hexagonal unit, and the assembled array may contain dozens or hundreds of hexagons (Figure 1). Each hexagonal unit is stabilized by a six-membered ring, composed of three kinase regulatory domains alternating with three CheW molecules, that contacts each of the six receptor oligomers within the hexagonal unit. This six-membered ring possesses pseudo-6-fold symmetry because of the homologous, dual-SH3 domain structural folds of the kinase regulatory domain and CheW.<sup>28,29</sup> The structural

framework of the array does not change substantially during ligand-triggered on–off switching; instead, signals are transmitted through the array by subtle structural and/or dynamical changes.<sup>31–38</sup>

The best studied chemosensory array is that of *Escherichia coli* and *Salmonella typhimurium*, two closely related species whose core array components are nearly identical and are functionally interchangeable.<sup>1,2,10,15,16</sup> Quantitative analysis of this array has revealed it is ultrasensitive, such that the binding of only one or two ligand molecules to the receptor lattice can generate a detectable signal output.<sup>39</sup> Moreover, *ex vivo* arrays assembled from the three core components in cells and isolated in bacterial membranes are kinetically ultrastable, such that upon incubation at room temperature the isolated arrays continue to exhibit receptor-regulated kinase activity for days or weeks.<sup>1</sup> The remarkable ultrasensitivity and ultrastability of the chemosensory array are believed to arise from an extensive network of contacts among the three core components.<sup>1,2,10</sup> These exceptional features, together with the availability of more than 20000 receptors specific for a wide array of ligands in bacterial genomes,<sup>40</sup> and the ability of receptors of different specificities to assemble into the same core units and arrays,<sup>27,41,42</sup> make the

Received: July 9, 2014

Published: August 13, 2014

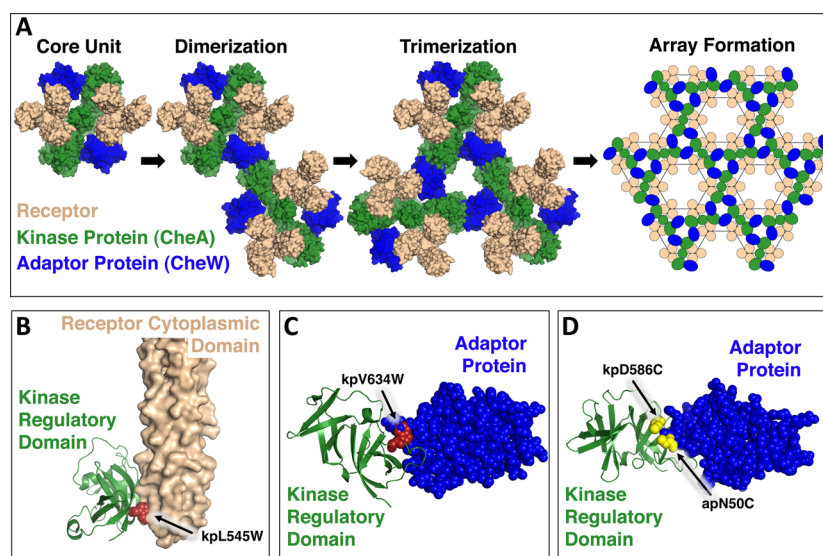


**Figure 1.** Core unit architecture, assembly of core units into higher-order complexes, and locations of the present modifications at specific core unit interfaces. (A) Current working model for the architecture of the core unit formed by two receptor oligomers (each a trimer of dimers, tan), one histidine kinase protein (CheA, a homodimer, green), and two adaptor proteins (CheW, monomeric, blue).<sup>14–22,24–27,43</sup> Shown also is the hypothesized mechanism for the assembly of core units into the hexagonal chemosensory array.<sup>43</sup> (B and C) Locations of the kinase regulatory domain bulky kpL545W and kpV634W Trp substitutions (brown) at the contacts with the receptor and adaptor protein, respectively.<sup>14–16</sup> (D) Location of the engineered kpD586C/apN50C Cys pair (yellow) at kinase–adaptor interface 1 in the kinase–adaptor ring.<sup>16</sup>

array a highly promising platform for the development of homogeneous and heterogeneous biosensors.

The receptor–kinase–adaptor core units, as well as larger assemblies of core units ranging in size up to small hexagonal arrays, can be reconstituted *in vitro* by combining isolated, receptor-containing bacterial membranes with purified kinase and adaptor protein.<sup>1,2,10,15,16,43–45</sup> Cryo-electron microscopy studies of reconstitutions in which the assembly process is halted before full array cooperativity is achieved, and presumably before the array is fully assembled, suggest the assembly reaction begins with the formation of individual core units, which then associate to form larger complexes, including dimers of core units (partial hexagons), trimers (full hexagons), and nascent arrays (multiple hexagons) (Figure 1A).<sup>43</sup> Like arrays isolated from cells, these reconstituted core complex preparations are kinetically ultra-stable at room temperature over a time scale of days to weeks.<sup>1,2</sup> When observed for several weeks, the kinase activity of the reconstituted core complexes decays as the bound kinase molecules are clipped by proteolysis, leading to the loss of the N-terminal substrate domain and kinase function.<sup>2</sup>

Careful analysis of the protein–protein interfaces that underlie the ultra-stability is central to a basic understanding of the conserved chemosensory array. Moreover, identification of the most crucial interfaces could lead to the development of new antibiotics that block pathogenic infection by disrupting the array and eliminating chemotaxis, rather than by destroying all pathogenic and nonpathogenic bacteria. Because the loss of chemosensing is detrimental only under nutrient-starved conditions,<sup>5,6,10,23,24</sup> antibiotics that disrupt the array would fight infection while preserving the microbiome important to human health.<sup>46,47</sup> Finally, interfacial modifications that enhance array stability could facilitate biosensor development.

Altogether, the chemosensory array is stabilized by four specific protein–protein contacts, two involving receptor contacts (with kinase and CheW) and two involving kinase–adaptor contacts within the six-membered ring (kinase–adaptor contacts 1 and 2, respectively).<sup>5,14,15,17–20</sup> This study inves-

tigated the contributions of two of the four interfaces: (i) the contact between the receptor protein interaction subdomain and the kinase regulatory domain that is formed within the core unit, and (ii) contact 1 between the kinase regulatory domain and the adaptor protein, which is also formed within the core unit. To destabilize or stabilize a given interface, the study employed a bulky Trp substitution to weaken the contact or an engineered disulfide bond to covalently bridge the interface, respectively. Subsequently, the effects of the modification on the kinetic stability and proteolytic susceptibility of the array proteins and their receptor-regulated kinase activity were quantified over long time courses extending for days or weeks. The findings show that both core unit interfaces examined play central roles in ultra-stability. Trp substitutions that weaken an interface reduce stability substantially, whereas a disulfide bond that covalently cross-links an interface dramatically enhances stability far beyond the already remarkable native ultra-stability.

## MATERIALS AND METHODS

**Materials.** All chemicals were highly pure reagent-grade. Chemicals were obtained from Sigma-Aldrich with the following exceptions: [ $\gamma$ -<sup>32</sup>P]ATP from PerkinElmer, dithiothreitol (DTT) from Research Products International, Ni-nitrilotriacetic acid (Ni-NTA) agarose resin from Qiagen, bicinchoninic acid assay (BCA) reagents from Bio-Rad, and polyvinylidene fluoride from Millipore.

**Protein Expression and Purification.** *S. typhimurium* Cysless CheA kinase and Cysless CheW adaptor protein possessing six-His tags on their N-termini were expressed from plasmids pET6H-CheA and pET6H-CheW, respectively, in *E. coli* strain BL21(DE3) (Stratagene).<sup>26</sup> The indicated CheA kinase and CheW adaptor protein point mutations were introduced into these Cysless backgrounds using the polymerase chain reaction-based QuickChange XLII mutagenesis kit (Agilent). Mutations were confirmed by DNA sequencing the coding region. *E. coli* CheY with a C-terminal six-His tag was

expressed by plasmid pVSCheY-6H in *E. coli* strain plasmid M15-pREP4 (Qiagen).<sup>36</sup> All soluble proteins were isolated as previously described by standard Ni-NTA agarose affinity chromatography.<sup>26,36</sup> Protein concentrations were estimated by UV absorption using extinction coefficients at 276 nm calculated from protein sequences as previously described.<sup>15</sup>

*E. coli* serine receptor (Tsr) was overexpressed in gutted *E. coli* strain UU1581, which lacks all chemotaxis proteins, including receptors and adaptation enzymes, using plasmid pJC3.<sup>42</sup> Inside out, inner bacterial membrane vesicles containing Tsr were isolated as previously described.<sup>26,48</sup> The total protein concentration in the membranes was determined by a BCA assay, and the fraction of total protein represented by receptors was determined by ImageJ densitometry of sodium dodecyl sulfate–polyacrylamide gel electrophoresis (SDS–PAGE) gels. The receptor concentration was determined by combining these two values.

**Reconstitution of Functional Core Complexes.** Functional, membrane-bound core complexes were reconstituted by combining 6.7  $\mu$ M Tsr receptor, 5  $\mu$ M CheA kinase, and 10  $\mu$ M CheW adaptor protein in kinase assay buffer [160 mM NaCl, 5 mM MgCl<sub>2</sub>, 50 mM Tris, 0.5 mM ethylenediaminetetraacetic acid (EDTA), pH 7.5] for 45 min at 22 °C in the presence of 0.5 mg/mL BSA, 2 mM TCEP, and 2 mM PMSF unless otherwise specified. Samples were centrifuged at 21000g for 7 min, and pellets were washed twice to remove free CheA kinase and CheW adaptor protein by being resuspended in a 10-fold excess of modified kinase assay buffer (without BSA, TCEP, and PMSF) and repelleted. After the final wash, pellets were resuspended in the original volume of modified kinase assay buffer, resulting in functional, washed core complexes.<sup>1,2</sup>

**Aging of Core Complexes.** Reconstituted, washed core complexes were aged as described with minor modifications.<sup>1,2</sup> Briefly, all Eppendorf tubes and pipet tips were autoclaved prior to being used, and an aseptic technique was utilized to minimize possible contamination. For each aging time course, reconstituted core complexes were incubated at room temperature (~22 °C) and protected from light for up to 432 h as specified. At each time point, the Eppendorf tubes containing the complexes were gently flicked to mix the membrane suspension, and then aliquots of the aged complexes were removed and prepared for quantification of the receptor-regulated CheA kinase activity and the amount of full-length CheA retained in the membrane complexes (see below).

Where specified, 3 nM trypsin (final concentration) was added immediately after core complex reconstitution as described previously<sup>2</sup> to ascertain whether the core components were susceptible to exogenous protease during the aging time course. Trypsin stocks were prepared fresh for each experiment from lyophilized powder and dissolved in 1 mM HCl at pH 3.

**Quantifying the Decay Kinetics of Receptor-Regulated CheA Kinase Activity within the Core Complexes.** To monitor the decay kinetics of CheA kinase activity, the relative kinase activities of core complexes were measured at time points during the aging time course, as previously described with minor modifications.<sup>26</sup> A 5  $\mu$ L aliquot of core complexes removed at a given time point was mixed with 5  $\mu$ L of CheY, yielding final concentrations of 3.3  $\mu$ M receptor and 40  $\mu$ M CheY. These concentrations were suitable to ensure that CheA kinase autophosphorylation was the rate-determining step and not phosphotransfer from CheA-P to CheY.<sup>49–51</sup> Receptor-mediated attractant regulation was quantified by addition of 2 mM serine. Kinase reactions were initiated by addition of 1 mM

[ $\gamma$ -<sup>32</sup>P]ATP (4000–8000 cpm/pmol), followed by reaction at 21 °C for 10 s, and then quenched by addition of 30  $\mu$ L of 2 $\times$  Laemmli sample buffer containing 50 mM EDTA. The samples were then snap-frozen in liquid nitrogen and stored at –20 °C until the time course was completed. All samples were then simultaneously analyzed on denaturing SDS–PAGE gels and extensively dried, and the  $\gamma$ -<sup>32</sup>P-labeled CheY band was quantified using phosphorimaging. The same stock of [ $\gamma$ -<sup>32</sup>P]ATP was utilized throughout the time course, ensuring that <sup>32</sup>P decay was equivalent for all samples and thus not a factor in time course analysis. Moreover, each gel included multiple aliquots of a large-volume, standard Cysless reaction conducted at the beginning of the time course and used to normalize the relative magnitudes of all  $\gamma$ -<sup>32</sup>P-labeled CheY bands on that gel, thereby correcting for minor variability between gels.

**Quantifying the Degradation Kinetics of Intact, Full-length CheA Kinase within the Core Complexes.** The time course of proteolytic degradation of intact, full-length CheA kinase within the reconstituted core complexes was quantified as described with minor modifications.<sup>1,2</sup> Briefly, 5  $\mu$ L of core complexes removed at a given time point was centrifuged at 21000g for 10 min to pellet the membranes, thereby separating them from any free CheA or fragments in solution. The supernatant was carefully removed by aspiration and the pellet resuspended in 10  $\mu$ L of sample loading buffer with or without DTT as indicated. The samples were then heated to 95 °C for 1 min, snap-frozen in liquid nitrogen, and finally stored at –80 °C until the time course was completed. Samples were then run on a 10% SDS gel to resolve the CheA kinase bands via Coomassie staining, and the full-length CheA band was quantified by densitometry. Each gel included multiple aliquots of a large-volume, standard Cysless core complex reconstitution conducted at the beginning of the time course and used to normalize the relative amounts of full-length CheA in all samples on the same gel, thereby correcting for minor variability between gels.

**Generating and Analyzing Disulfide-Linked, Reconstituted Core Complexes.** Reconstituted core complexes containing disulfide-linked CheA kinase and CheW adaptor protein were generated using a modified reconstitution procedure as described previously.<sup>16</sup> Briefly, core components were mixed together as described above, except that no reducing agents were utilized. After the 45 min incubation, Cu(II) was added to a final concentration of 5 mM. After 20 s, 2 volumes of kinase assay buffer was added, and the membrane-bound core complexes were immediately washed to remove any unbound CheA kinase and CheW adaptor protein as well as Cu(II). The decay of kinase activity and the decay of full-length CheA kinase were quantified during aging of the core complexes as described above.

**Data and Error Analysis.** All data points shown are averages of a minimum of three replicates. Error bars and ranges indicate the standard error unless otherwise specified. Asterisks indicate statistically significant changes ( $P < 0.05$ ).

## RESULTS

**Modified Core Proteins Employed in This Study.** To test the effects of perturbing two key protein–protein interfaces within the core unit on the ultrastability of reconstituted core complexes, four previously described<sup>15,16</sup> mutations were introduced into the standard set of Cysless core proteins. These core proteins were the natively Cysless serine receptor (Tsr) and engineered Cysless versions of CheA His-kinase and CheW adaptor protein, which together are known to yield



**Table 1. Functional Parameters of Reconstituted Core Complexes**

kinase and adaptor proteins <sup>a</sup>	kinase incorporation <sup>b</sup>	kinase specific activity <sup>c</sup>	
		without Ser	with Ser
kp and ap Cysless	1.0 ± 0.1	1.0 ± 0.1	0.05 ± 0.01
kpL545W, apCysless <sup>d</sup>	0.9 ± 0.2	0.20 ± 0.02	0.01 ± 0.01
kpV634W, apCysless <sup>e</sup>	0.6 ± 0.1	0.5 ± 0.1	0.08 ± 0.1
kpD586C, apN50C (reduced) <sup>e</sup>	1.0 ± 0.2	1.0 ± 0.2	0.2 ± 0.1
kpD586C–apN50C (oxidized) <sup>e</sup>	1.0 ± 0.2	1.1 ± 0.1	0.2 ± 0.1

<sup>a</sup>kp, kinase protein (CheA); ap, adaptor protein (CheW). <sup>b</sup>Relative to Cysless. <sup>c</sup>Relative to Cysless without Ser. <sup>d</sup>Also see ref 15. <sup>e</sup>Also see ref 16.

functional, ultrastable core complexes.<sup>1,2</sup> Figure 1 illustrates the locations of the four interface-perturbing modifications within the core complex.

**Effects of the Modified Proteins on the Assembly and Kinase Activity of Reconstituted Core Complexes.** At the receptor–kinase interface, the kinase protein L545W mutation (kpL545W)<sup>15</sup> was designed to weaken the primary receptor–kinase contact by introducing a surface Trp substitution onto the receptor-binding face of the kinase P5 regulatory domain (Figure 1B). The bulky Trp side chain at this position had little or no effect on the level of kinase incorporated into core complexes during reconstitution but significantly reduced the specific activity of the incorporated kinase (ref 15 and Table 1). The latter inhibition of specific kinase activity indicates a loss of receptor-mediated kinase activation within the assembled core complexes. The minor effect on kinase incorporation suggests that the assembly reaction is directed largely by one or more of the other three contacts, rather than by the receptor–kinase contact.

At the kinase–adaptor interface within the core unit (kinase–adaptor contact 1), the kinase protein V634W mutation (kpV634W)<sup>16</sup> was designed to introduce a bulky surface Trp onto the surface of the kinase P5 regulatory domain that contacts the adaptor protein (Figure 1C). The mutation was observed to significantly reduce both the level of incorporation of kinase into the reconstituted complexes and the specific kinase activity of the molecules that are incorporated (ref 16 and Table 1), indicating that kinase–adaptor contact 1 is important in both complex assembly and kinase function.

At this same kinase–adaptor contact 1, the kinase protein mutation D586C (kpD586C) and the adaptor protein mutation N50C (apN50C) together introduced a pair of surface Cys residues separated by only 7 Å that were easily oxidized to form an interface-bridging disulfide bond within the core unit<sup>16</sup> (Figure 1D). The reduced Cys pair was relatively nonperturbing, yielding near-native kinase incorporation and specific activity in reconstituted core complexes. Furthermore, disulfide formation within the assembled complexes retained full kinase activity, indicating the disulfide bond covalently stabilized the native interface (ref 16 and Table 1). [Note that analogous engineered disulfide studies of the receptor–kinase interface were not possible, because only two of the six receptor homodimers in the core unit are bound to the kinase (Figure 1A). As previously observed, oxidation of complexes possessing Cys pairs on the receptor and kinase yielded extensive receptor–receptor disulfide cross-linking that destroyed the native structure and kinase activity of the reconstituted core complexes.<sup>15]</sup>

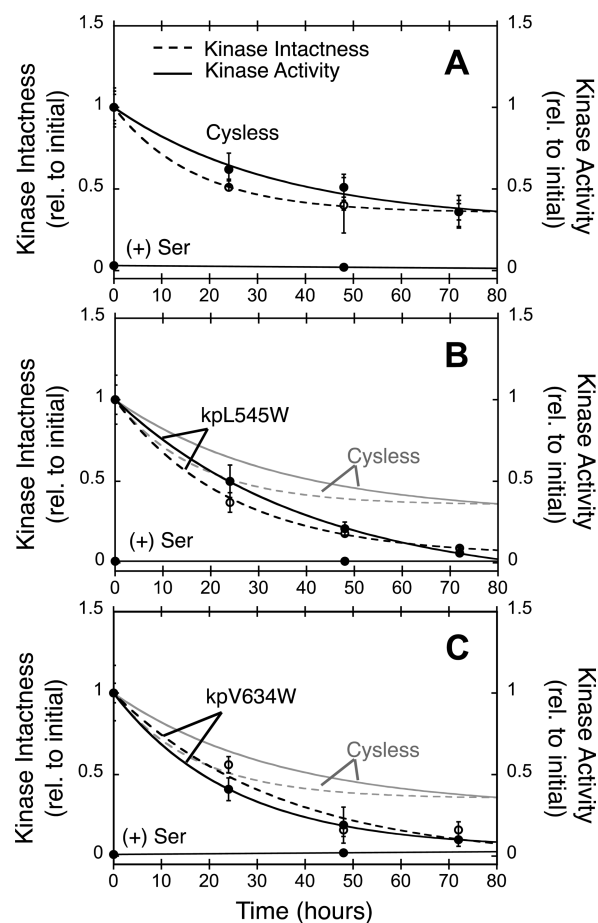


**Figure 2.** Effect of bulky kpL545W and kpV634W Trp substitutions on the ultrastability of reconstituted core complexes. Shown are 72 h decay time courses for reconstituted, washed core complexes formed on isolated *E. coli* membranes. Serine receptor (Tsr), histidine kinase (CheA), and adaptor protein (CheW) were mixed and incubated to reconstitute core complexes, and then the resulting membrane-bound complexes were washed to remove unbound components. Each plot summarizes the decay of intact, full-length kinase (Kinase Intactness, dashed line and empty symbols) and of kinase enzymatic function (Kinase Activity, solid line and filled symbols). In each case, the addition of attractant (Ser) fully inhibited kinase activity via native, receptor-mediated kinase regulation. Table 2 summarizes the kinetic parameters for each time course. (A) Decay of control Cysless reconstituted complexes, exhibiting both a quasi-stable component ( $\tau = 17\text{--}34$  h for 60–70% of the population) and an ultrastable component ( $\tau \gg 72$  h for the remaining 30–40% of the population). (B) Decay of reconstituted complexes containing the kinase protein kpL545W mutation to perturb the receptor–kinase interface within the core unit, exhibiting a quasi-stable ( $\tau = 24\text{--}41$  h for 100% of the population) but no ultrastable component. (C) Decay of reconstituted complexes containing the kinase protein kpV634W mutation to perturb kinase–adaptor protein interface 1, located within the core unit. The decay exhibits a quasi-stable ( $\tau = 25\text{--}35$  h for 100% of the population) but no ultrastable component.

**Effects of Bulky Trp Substitutions on the Stability of Reconstituted Core Complexes.** To test the prediction that ultrastability requires the native receptor–kinase and kinase–adaptor contacts within the core unit, the stabilities of core complexes reconstituted from Cysless and Trp mutant components were compared in 72 h time courses. The decay of both (i) intact, core complex-associated, full-length kinase protein and (ii) total, core complex-associated kinase activity was quantified. For the control Cysless reconstituted complexes, as

Table 2. Decay Kinetics of Native and Modified Reconstituted Core Complexes

kinase and adaptor proteins <sup>b</sup>	For 72 h Time Courses <sup>a</sup> [ $f(x) = Ae^{-t/\tau} + C$ ]					
	activity A	activity $\tau$ (h)	activity C	intactness A	intactness $\tau$ (h)	intactness C
kp and ap Cysless, reduced	0.7 ± 0.1	34 ± 10	0.3 ± 0.1	0.6 ± 0.1	17 ± 1	0.4 ± 0.1
kp and ap Cysless, oxidized	0.7 ± 0.1	32 ± 9	0.3 ± 0.1	0.7 ± 0.1	19 ± 1	0.3 ± 0.1
kpL545W, apCysless	1.0 ± 0.1	41 ± 1	0.0 ± 0.1	1.0 ± 0.1	24 ± 3	0.0 ± 0.1
kpV634W, apCysless	1.0 ± 0.1	35 ± 9	0.0 ± 0.1	1.0 ± 0.1	25 ± 7	0.0 ± 0.1
kpD586C, apN50C, reduced	0.8 ± 0.1	36 ± 6	0.2 ± 0.1	0.6 ± 0.1	21 ± 8	0.4 ± 0.1
kpD586C, apN50C, oxidized	1.0	>300	0.0	1.0	>300	0.0

kinase and adaptor proteins <sup>b</sup>	For 432 h Time Courses <sup>a</sup> [ $f(x) = A_{\text{fast}}e^{-t/\tau_{\text{fast}}} + A_{\text{slow}}e^{-t/\tau_{\text{slow}}}$ ]							
	activity $A_{\text{fast}}$	activity $\tau_{\text{fast}}$ (h)	activity $A_{\text{slow}}$	activity $\tau_{\text{slow}}$ (h)	intactness $A_{\text{fast}}$	intactness $\tau_{\text{fast}}$ (h)	intactness $A_{\text{slow}}$	intactness $\tau_{\text{slow}}$ (h)
kp and ap Cysless, reduced	0.50 ± 0.01	35 ± 5	0.50 ± 0.02	440 ± 40	0.50 ± 0.01	42 ± 5	0.50 ± 0.01	750 ± 40
kpD586C, apN50C, oxidized	0.0	not applicable	1.0	>>1000	0.0	not applicable	1.0	>>1000

<sup>a</sup>Decay time course of kinase activity or intactness. <sup>b</sup>kp, kinase protein (CheA); ap, adaptor protein (CheW).

previously observed,<sup>2</sup> the decays of kinase intactness and activity each displayed two-component decay time courses in which (i) the quasi-stable component (approximately half of the observed population) was lost over the 72 h experiment with an exponential decay time of 17–34 h whereas (ii) the ultrastable component (the remaining half) remained intact after 72 h (Figure 2A and Table 2). Longer time courses have previously shown that the ultrastable component exhibits an exponential decay time of weeks rather than days (ref 2 and Figure 3C).

In contrast to the two-component decays of the control core complexes, the decay time courses of core complexes containing either one of the two interfacial Trp substitutions possessed only one component because the ultrastable subpopulation was converted to the quasi-stable state. Incorporation of either bulky Trp yielded a single population of reconstituted complexes exhibiting an exponential decay time of 24–41 h that was the same, within error, as that observed for the quasi-stable component of control Cysless complexes (Figure 2B,C and Table 2).

The lack of an ultrastable component in these mutant complexes strongly supports the hypothesis that the native receptor–kinase and kinase–adaptor core unit interfaces both play essential roles in ultrastability. These findings are consistent with the previous observation that coupling a bulky fluor to the receptor protein interaction region eliminates ultrastability, by disrupting the receptor–kinase interface as described above, by disrupting the receptor–adaptor protein interface, or both because the homologous kinase P5 regulatory domain and the adaptor protein bind to the same site on different receptor molecules.<sup>2</sup>

**Effects of an Interfacial Disulfide Bond on the Stability of Reconstituted Core Complexes.** To ascertain whether additional stabilization of a specific protein–protein contact can further enhance the stability of reconstituted core complexes, the stabilities of reconstituted core complexes lacking and possessing the engineered kpD586C–apN50C disulfide bond bridging kinase–adaptor contact 1 were quantified. The control experiment depicted in Figure 3A shows that the reduction and oxidation conditions used in these studies to generate the fully reduced Cys pair and the disulfide bond, respectively, had little or no effect on the stability of reconstituted Cysless complexes.

Strikingly, oxidative formation of the interfacial, kpD586C–apN50C disulfide bond converted the quasi-stable population to the ultrastable state and dramatically enhanced the stability of the reconstituted core complex. The oxidized disulfide-containing

core complexes exhibited little loss of intact, full-length kinase, and minimal loss of specific kinase activity, relative to those of Cysless or reduced di-Cys complexes lacking the disulfide bond over the 72 h time course (Figure 3B and Table 2).

The enhanced stability conferred by the disulfide bond necessitated a longer time scale measurement to quantify the decay lifetime. Thus, a 432 h time course was conducted, which revealed that the disulfide-containing core complexes behaved like a single population in which the exponential decay constant for the loss of intact, full-length kinase, or its activity, greatly exceeded 1000 h (or 5.9 weeks) (Figure 3C and Table 2). In contrast, Cysless complexes lacking the disulfide displayed both quasi-stable and ultrastable components of equal proportions with decay times (35–42 and 440–750 h, respectively) similar to those previously measured on long time scales (ref 2, Figure 3C, and Table 2).

Previous studies have shown that the more rapid decay of the quasi-stable state in reconstituted core complexes arises from proteolysis of the bound kinase at its P1–P2 or P2–P3 linker. Both of these long linkers couple the P1 substrate domain to the P3–P4–P5 kinase core region, and both are susceptible to proteolysis in the free kinase. Proteolysis of either linker releases the substrate domain while the P2–P3–P4–P5 or P3–P4–P5 fragment remains bound in the core complex, leading to loss of both intact, full-length kinase and kinase activity.<sup>2</sup> Thus, the simplest hypothesis for the stabilizing mechanism of the disulfide linkage is protection of the bound kinase against proteolysis.

**Testing the Hypothesis That the Stability-Enhancing Disulfide Protects Reconstituted Core Complexes from Proteolysis.** To test the ability of the stabilizing kpD586C–apN50C disulfide bond to protect reconstituted complexes against proteolysis, the stabilities of complexes lacking and possessing the disulfide were quantified in the presence of added trypsin. As previously observed,<sup>2</sup> a low level of exogenous trypsin (3 nM) sped the decay of intact, full-length kinase and kinase activity for the quasi-stable component of Cysless complexes over a 24 h time course but had little or no effect on the ultrastable component (Figure 4A and Table 3). Similarly, trypsin accelerated the decay of the quasi-stable component, but not the ultrastable component, of reduced di-Cys complexes (Figure 4B and Table 3). The same level of trypsin had little or no effect on reconstituted, disulfide-containing complexes, indicating virtually complete protection from proteolysis over the 24 h time course (Figure 4B and Table 3). This full protection

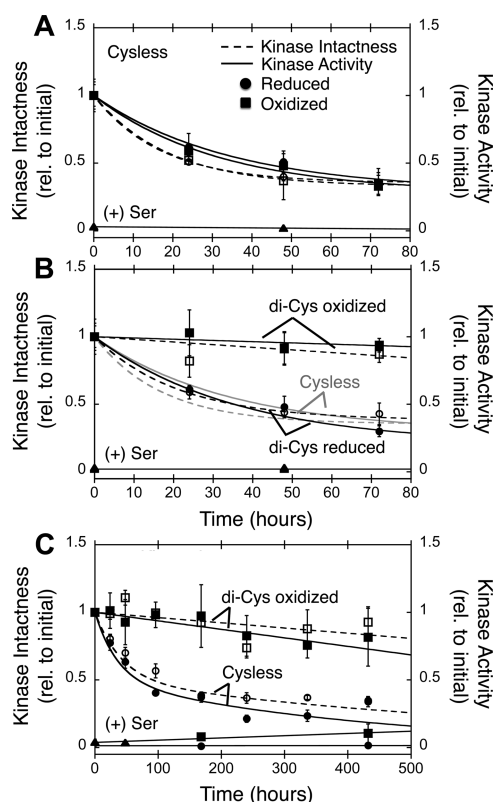


**Figure 3.** Effects on ultrastability of a disulfide bond bridging a core unit interface. Decay time courses for reconstituted and washed core complexes are shown (see the legend of Figure 2). These decays demonstrate the effects of the reduced or oxidized kpD586C/apN50C Cys pair at kinase–adaptor interface 1 within the core unit; the kpD586C–apN50C disulfide covalently cross-links this interface.<sup>16</sup> Each plot summarizes the decay of intact, full-length kinase (Kinase Intactness, dashed line and empty symbols) and of kinase enzymatic function (Kinase Activity, solid line and filled symbols). Addition of attractant (Ser) is observed to fully inhibit kinase activity via native receptor-mediated kinase regulation. Table 2 summarizes the kinetic parameters. (A) A 72 h decay time course of control reconstituted Cysless complexes, showing that the redox treatments yield minimal perturbation of the decay kinetics (compare with Figure 2A and Table 2). Both the reduced and oxidized complexes exhibit a quasi-stable component ( $\tau = 17\text{--}34$  and  $19\text{--}32$  h, respectively, for 60–70% of the population) and an ultrastable component ( $\tau \gg 72$  h for 30–40% of the population). (B) A 72 h time course of the decay of reconstituted di-Cys complexes containing the reduced Cys pair or the oxidized disulfide linkage. The reduced di-Cys complexes exhibit both a quasi-stable component ( $\tau = 21\text{--}36$  h for 60–80% of the population) and an ultrastable component ( $\tau \gg 72$  h for 20–40% of the population) as observed in panel A for native Cysless complexes. In contrast, the oxidized di-Cys complexes exhibit only the ultrastable component ( $\tau > 300$  h for 100% of the population). (C) A 432 h time course comparing the decay of Cysless complexes to that of oxidized di-Cys complexes containing the disulfide linkage. As usual, the Cysless complexes exhibit both a quasi-stable component ( $\tau = 35\text{--}42$  h for 50% of the population) and an ultrastable component ( $\tau = 440\text{--}750$  h for 50% of the population). In contrast, the oxidized di-Cys complexes exhibit only the ultrastable component ( $\tau \gg 1000$  h for 100% of the population).

provides further evidence that the disulfide drives the entire core complex population into the ultrastable state.

## DISCUSSION

The findings reveal that a bulky surface Trp substitution at either of two key core unit interfaces, the receptor–kinase interface or

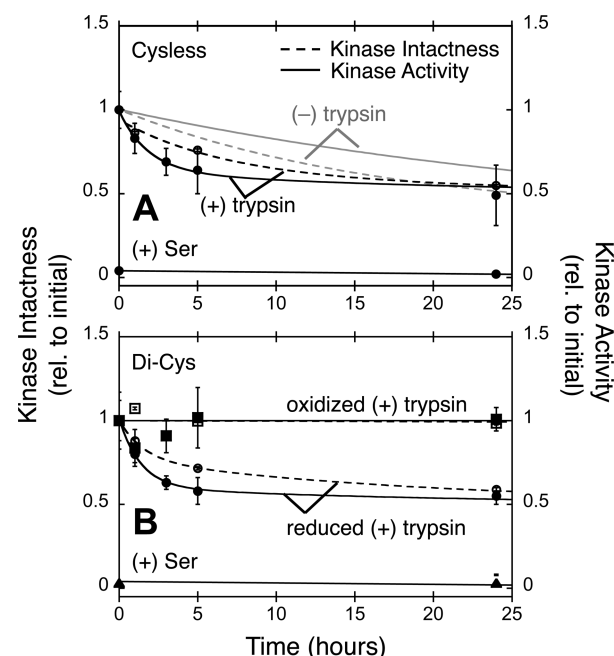


**Figure 4.** Effect of a disulfide bond bridging a core unit interface on susceptibility to proteolysis. A 24 h time course illustrating the effects of added trypsin on Cysless and di-Cys complexes possessing the kpD586C/apN50C Cys pair (see the legends of Figures 2 and 3). Each plot summarizes the decay of intact, full-length kinase (Kinase Intactness, dashed line and empty symbols) and of kinase enzyme activity (Kinase Activity, solid line and filled symbols). Addition of attractant (Ser) is observed to fully inhibit, within error, receptor-mediated stimulation of kinase activity. Table 3 summarizes the kinetic parameters. (A) Decay time courses of control, reconstituted Cysless complexes showing that in the absence of trypsin the decay exhibits the usual quasi-stable ( $\tau = 35\text{--}42$  h for 50% of the population) and ultrastable ( $\tau \gg 42$  h for 50% of the population) components. Trypsin speeds the decay of most of the quasi-stable component ( $\tau = 1.8\text{--}6.3$  h for 30–40% of the population, and  $\tau = 35\text{--}42$  h for 10–20% of the population), whereas trypsin has no detectable effect on the ultrastable component ( $\tau \gg 48$  h for 50% of the population). (B) Decay time course of reconstituted di-Cys complexes containing the reduced Cys pair or the oxidized disulfide linkage, both in the presence of trypsin. For reduced di-Cys complexes, as for Cysless complexes (see panel A), trypsin speeds the decay of most of the quasi-stable component ( $\tau = 1.4\text{--}1.5$  h for 20–40% of the population, and  $\tau = 35\text{--}42$  h for 10–30% of the population), whereas trypsin has no detectable effect on the ultrastable component ( $\tau \gg 48$  h for 50% of the population). In striking contrast, the oxidized di-Cys complexes possess no detectable quasi-stable component, and the ultrastable component is fully resistant to trypsin on the examined time scale ( $\tau \gg 48$  h for 100% of the population).

kinase–adaptor interface 1, eliminates the ultrastability of reconstituted core complexes (Figure 2 and Table 2). It follows that both native interfaces play essential roles in ultrastability and that a single modification at either site can disrupt this unique property, yet these same Trp substitutions allow near normal core complex assembly and have little or no effect on the decay kinetics of the quasi-stable state, indicating those features are less sensitive to perturbations and do not require a full set of native core unit contacts. More generally, the quasi-stable and ultrastable states of native reconstituted complexes exhibit indistinguishable specific kinase activities and attractant regulation. Thus, the key features of the quasi-stable state that distinguish it from the ultrastable state are its shorter functional



**Table 3. Decay Kinetics of Native and Modified Reconstituted Core Complexes and Effects of Exogenous Protease**

kinase (and adaptor) proteins <sup>b</sup>	For 24 h Time Courses <sup>a</sup> [ $f(x) = A_{\text{trypsin}}e^{-t/\tau_{\text{trypsin}}} + A_{\text{fast}}e^{-t/\tau_{\text{fast}}} + C$ (where $\tau_{\text{fast}}$ is the Cysless value and $C = 0.5$ )]									
	activity $A_{\text{trypsin}}$	activity $\tau_{\text{trypsin}}$ (h)	activity $A_{\text{fast}}$	activity $\tau_{\text{fast}}$ (h)	activity $C$	intactness $A_{\text{trypsin}}$	intactness $\tau_{\text{trypsin}}$ (h)	intactness $A_{\text{fast}}$	intactness $\tau_{\text{fast}}$ (h)	intactness $C$
kp and ap Cysless, reduced (–) trypsin	not available	not available	0.50 ± 0.01	35 ± 5	0.50 ± 0.02	no data	no data	0.50 ± 0.01	42 ± 5	0.50 ± 0.03
kp and ap Cysless, reduced (+) trypsin	0.4 ± 0.1	1.8 ± 0.7	0.1 ± 0.1	(35)	(0.5)	0.3 ± 0.1	6.3 ± 0.9	0.2 ± 0.1	(42)	(0.5)
kpD586C, apN50C, reduced (+) trypsin	0.4 ± 0.1	1.4 ± 0.9	0.1 ± 0.1	(35)	(0.5)	0.2 ± 0.1	1.5 ± 0.4	0.3 ± 0.1	(42)	(0.5)
kpD586C–apN50C, oxidized (+) trypsin	0.0	not applicable	0.0	not applicable	1.0	0.0	not applicable	0.0	not applicable	1.0

<sup>a</sup>Decay time course of kinase activity or intactness. <sup>b</sup>kp, kinase protein (CheA); ap, adaptor protein (CheW).

lifetime and its lack of sensitivity to interfacial mutations (Table 2). A simple hypothesis consistent with these observations is that the fully functional, quasi-stable state is formed early in the assembly reaction, whereas the ultrastable state is formed later by the establishment of additional, or more well-ordered, protein–protein contacts.

Strong evidence supporting the role of well-formed interfaces in the ultrastable state is provided by the discovery that an engineered disulfide bond greatly enhances ultrastability. This disulfide bridges core unit kinase–adaptor interface 1 and generates virtually complete conversion of the quasi-stable state into the ultrastable state, while also doubling the already remarkable persistence of the ultrastable state (Figure 3 and Table 2). The resulting enhancement of stability increases the functional, exponential lifetime of the ultrastable state from 460 ± 50 h (19 days) to well over 1000 h (a lower limit, approximately 6 weeks).

The findings also reveal that the interfacial disulfide enhances ultrastability by protecting the bound kinase from proteolysis. Previous studies have shown that, in the quasi-stable state, the decay of intact, full-length kinase and its activity arises from an endogenous protease activity that clips the bound kinase at the long linkers connecting the P1 substrate domain and the P2 response regulator-binding domain to the core of the kinase molecule.<sup>2</sup> Moreover, the addition of trypsin was found to speed proteolysis of the kinase in the quasi-stable state while having little or no effect on the ultrastable state. The present findings show that when the interfacial disulfide converts the entire population to the ultrastable state, it protects the entire population from both endogenous protease and exogenous trypsin (Figure 4 and Table 3).

The simplest model for explaining these properties is that in which proteolysis occurs when structural fluctuations within the reconstituted complex expose the long linkers of the kinase substrate domain to the endogenous or exogenous protease, whereas protection against proteolysis either decreases the dynamics or increases the level of steric protection of these linkers. Further studies are needed to ascertain whether the disulfide-driven protection is provided simply by local stabilization within individual core units via covalent cross-linking of its kinase–adaptor interface, or rather by driving the assembly of core units into larger complexes in which the local lattice architecture shields the kinase from protease. Either mechanism is possible, because the disulfide-stabilized interface is located within, rather than between, core units, but stabilization of the native core unit structure could increase the density of assembled core units on the membrane and thereby shift the equilibrium toward assembly of larger core unit oligomers and arrays.

Finally, the observation that different interfacial modifications can either eliminate or enhance ultrastability suggests that native ultrastability is an evolved trait that provides an optimal, rather than the maximal, level of kinetic durability. In this picture, new selective pressures could either increase or decrease this durability. Because the ultrastability and long-range cooperativity of the chemosensory array are linked by their codependence on connectivity between components, and because both are needed for optimal chemotaxis and survival under nutrient-limited conditions, these two properties may well exhibit co-evolution. Our findings raise the possibility that some as yet uncharacterized bacterial chemotaxis pathways may utilize disulfide bonds to generate very long-lived, highly cooperative chemosensory arrays. These findings also provide a new impetus for using the bacterial chemosensory array as a platform for the development of ultrasensitive, ultrastable biosensors.

## AUTHOR INFORMATION

### Corresponding Author

\*E-mail: falke@colorado.edu. Telephone: (303) 492-3503.

### Funding

Support provided by National Institutes of Health Grant R01 GM-040731 (to J.J.F.).

### Notes

The authors declare no competing financial interest.

## ACKNOWLEDGMENTS

We gratefully acknowledge Marc-Andre LeBlanc for expert technical assistance on preliminary studies of trypsin sensitivity.

## REFERENCES

- (1) Erbs, A. H., and Falke, J. J. (2009) The core signaling proteins of bacterial chemotaxis assemble to form an ultrastable complex. *Biochemistry* 48, 6975–6987.
- (2) Slivka, P. F., and Falke, J. J. (2012) Isolated Bacterial Chemosensory Array Possesses Quasi- and Ultrastable Components: Functional Links between Array Stability, Cooperativity, and Order. *Biochemistry* 51, 10218–10228.
- (3) Briegel, A., Ladinsky, M. S., Oikonomou, C., Jones, C. W., Harris, M. J., Fowler, D. J., Chang, Y. W., Thompson, L. K., Armitage, J. P., and Jensen, G. J. (2014) Structure of bacterial cytoplasmic chemoreceptor arrays and implications for chemotactic signaling. *Elife* 3, e02151.
- (4) Tu, Y. (2013) Quantitative modeling of bacterial chemotaxis: Signal amplification and accurate adaptation. *Annu. Rev. Biophys.* 42, 337–359.
- (5) Sourjik, V., and Wingreen, N. S. (2012) Responding to chemical gradients: Bacterial chemotaxis. *Curr. Opin. Cell Biol.* 24, 262–268.
- (6) Hazelbauer, G. L. (2012) Bacterial chemotaxis: The early years of molecular studies. *Annu. Rev. Microbiol.* 66, 285–303.

- (7) Porter, S. L., Wadhams, G. H., and Armitage, J. P. (2011) Signal processing in complex chemotaxis pathways. *Nat. Rev. Microbiol.* 9, 153–165.
- (8) Miller, J., Parker, M., Bourret, R. B., and Giddings, M. C. (2010) An agent-based model of signal transduction in bacterial chemotaxis. *PLoS One* 5, e9454.
- (9) Bourret, R. B., and Silversmith, R. E. (2010) Two-component signal transduction. *Curr. Opin. Microbiol.* 13, 113–115.
- (10) Hazelbauer, G. L., Falke, J. J., and Parkinson, J. S. (2008) Bacterial chemoreceptors: High-performance signaling in networked arrays. *Trends Biochem. Sci.* 33, 9–19.
- (11) Chaparro, A. P., Ali, S. K., and Klose, K. E. (2010) The ToxT-dependent methyl-accepting chemoreceptors AcfB and TcpI contribute to *Vibrio cholerae* intestinal colonization. *FEMS Microbiol. Lett.* 302, 99–105.
- (12) Ratterman, E. L., and Welch, R. A. (2013) Chemoreceptors of *Escherichia coli* CFT073 play redundant roles in chemotaxis toward urine. *PLoS One* 8, e54133.
- (13) Grim, C. J., Kozlova, E. V., Sha, J., Fitts, E. C., van Lier, C. J., Kirtley, M. L., Joseph, S. J., Read, T. D., Burd, E. M., Tall, B. D., Joseph, S. W., Horneman, A. J., Chopra, A. K., and Shak, J. R. (2013) Characterization of *Aeromonas hydrophila* wound pathotypes by comparative genomic and functional analyses of virulence genes. *MBio* 4, e00064-13.
- (14) Li, X., Fleetwood, A. D., Bayas, C., Bilwes, A. M., Ortega, D. R., Falke, J. J., Zhulin, I. B., and Crane, B. R. (2013) The 3.2 Å Resolution Structure of a Receptor:CheA:CheW Signaling Complex Defines Overlapping Binding Sites and Key Residue Interactions within Bacterial Chemosensory Arrays. *Biochemistry* 52, 3852–3865.
- (15) Piasta, K. N., Ulliman, C. J., Slivka, P. F., Crane, B. R., and Falke, J. J. (2013) Defining a Key Receptor-CheA Kinase Contact and Elucidating Its Function in the Membrane-Bound Bacterial Chemosensory Array: A Disulfide Mapping and TAM-IDS Study. *Biochemistry* 52, 3866–3880.
- (16) Natale, A. M., Duplantier, J. L., Piasta, K. N., and Falke, J. J. (2013) Structure, function, and on-off switching of a core unit contact between CheA kinase and CheW adaptor protein in the bacterial chemosensory array: A disulfide mapping and mutagenesis study. *Biochemistry* 52, 7753–7765.
- (17) Briegel, A., Li, X., Bilwes, A. M., Hughes, K. T., Jensen, G. J., and Crane, B. R. (2012) Bacterial chemoreceptor arrays are hexagonally packed trimers of receptor dimers networked by rings of kinase and coupling proteins. *Proc. Natl. Acad. Sci. U.S.A.* 109, 3766–3771.
- (18) Liu, J., Hu, B., Morado, D. R., Jani, S., Manson, M. D., and Margolin, W. (2012) Molecular architecture of chemoreceptor arrays revealed by cryoelectron tomography of *Escherichia coli* minicells. *Proc. Natl. Acad. Sci. U.S.A.* 109, E1481–E1488.
- (19) Wang, X., Vu, A., Lee, K., and Dahlquist, F. W. (2012) CheA-receptor interaction sites in bacterial chemotaxis. *J. Mol. Biol.* 422, 282–290.
- (20) Vu, A., Wang, X., Zhou, H., and Dahlquist, F. W. (2012) The receptor-CheW binding interface in bacterial chemotaxis. *J. Mol. Biol.* 415, 759–767.
- (21) Li, M., and Hazelbauer, G. L. (2011) Core unit of chemotaxis signaling complexes. *Proc. Natl. Acad. Sci. U.S.A.* 108, 9390–9395.
- (22) Li, M., Khursigara, C. M., Subramaniam, S., and Hazelbauer, G. L. (2011) Chemotaxis kinase CheA is activated by three neighbouring chemoreceptor dimers as effectively as by receptor clusters. *Mol. Microbiol.* 79, 677–685.
- (23) Wuichet, K., and Zhulin, I. B. (2010) Origins and diversification of a complex signal transduction system in prokaryotes. *Sci. Signaling* 3, ra50.
- (24) Briegel, A., Ortega, D. R., Tocheva, E. I., Wuichet, K., Li, Z., Chen, S., Muller, A., Iancu, C. V., Murphy, G. E., Dobro, M. J., Zhulin, I. B., and Jensen, G. J. (2009) Universal architecture of bacterial chemoreceptor arrays. *Proc. Natl. Acad. Sci. U.S.A.* 106, 17181–17186.
- (25) Zhang, P., Khursigara, C. M., Hartnell, L. M., and Subramaniam, S. (2007) Direct visualization of *Escherichia coli* chemotaxis receptor arrays using cryo-electron microscopy. *Proc. Natl. Acad. Sci. U.S.A.* 104, 3777–3781.
- (26) Miller, A. S., Kohout, S. C., Gilman, K. A., and Falke, J. J. (2006) CheA Kinase of bacterial chemotaxis: Chemical mapping of four essential docking sites. *Biochemistry* 45, 8699–8711.
- (27) Studdert, C. A., and Parkinson, J. S. (2004) Crosslinking snapshots of bacterial chemoreceptor squads. *Proc. Natl. Acad. Sci. U.S.A.* 101, 2117–2122.
- (28) Griswold, I. J., Zhou, H., Matison, M., Swanson, R. V., McIntosh, L. P., Simon, M. I., and Dahlquist, F. W. (2002) The solution structure and interactions of CheW from *Thermotoga maritima*. *Nat. Struct. Biol.* 9, 121–125.
- (29) Bilwes, A. M., Alex, L. A., Crane, B. R., and Simon, M. I. (1999) Structure of CheA, a signal-transducing histidine kinase. *Cell* 96, 131–141.
- (30) Kim, K. K., Yokota, H., and Kim, S. H. (1999) Four-helical-bundle structure of the cytoplasmic domain of a serine chemotaxis receptor. *Nature* 400, 787–792.
- (31) Wang, X., Vallurupalli, P., Vu, A., Lee, K., Sun, S., Bai, W. J., Wu, C., Zhou, H., Shea, J. E., Kay, L. E., and Dahlquist, F. W. (2014) The linker between the dimerization and catalytic domains of the CheA histidine kinase propagates changes in structure and dynamics that are important for enzymatic activity. *Biochemistry* 53, 855–861.
- (32) Briegel, A., Ames, P., Gumbart, J. C., Oikonomou, C. M., Parkinson, J. S., and Jensen, G. J. (2013) The mobility of two kinase domains in the *Escherichia coli* chemoreceptor array varies with signaling state. *Mol. Microbiol.* 89, 831–841.
- (33) Sferdean, F. C., Weis, R. M., and Thompson, L. K. (2012) Ligand affinity and kinase activity are independent of bacterial chemotaxis receptor concentration: Insight into signaling mechanisms. *Biochemistry* 51, 6920–6931.
- (34) Briegel, A., Beeby, M., Thanbichler, M., and Jensen, G. J. (2011) Activated chemoreceptor arrays remain intact and hexagonally packed. *Mol. Microbiol.* 82, 748–757.
- (35) Zhou, Q., Ames, P., and Parkinson, J. S. (2011) Biphasic control logic of HAMP domain signalling in the *Escherichia coli* serine chemoreceptor. *Mol. Microbiol.* 80, 596–611.
- (36) Miller, A. S., and Falke, J. J. (2004) Side chains at the membrane-water interface modulate the signaling state of a transmembrane receptor. *Biochemistry* 43, 1763–1770.
- (37) Isaac, B., Gallagher, G. J., Balazs, Y. S., and Thompson, L. K. (2002) Site-directed rotational resonance solid-state NMR distance measurements probe structure and mechanism in the transmembrane domain of the serine bacterial chemoreceptor. *Biochemistry* 41, 3025–3036.
- (38) Falke, J. J., and Hazelbauer, G. L. (2001) Transmembrane signaling in bacterial chemoreceptors. *Trends Biochem. Sci.* 26, 257–265.
- (39) Sourjik, V., and Berg, H. C. (2002) Receptor sensitivity in bacterial chemotaxis. *Proc. Natl. Acad. Sci. U.S.A.* 99, 123–127.
- (40) Wilson, D., Pethica, R., Zhou, Y., Talbot, C., Vogel, C., Madera, M., Chothia, C., and Gough, J. (2009) SUPERFAMILY: Sophisticated comparative genomics, data mining, visualization and phylogeny. *Nucleic Acids Res.* 37, D380–D386.
- (41) Parkinson, J. S., Ames, P., and Studdert, C. A. (2005) Collaborative signaling by bacterial chemoreceptors. *Curr. Opin. Microbiol.* 8, 116–121.
- (42) Ames, P., Studdert, C. A., Reiser, R. H., and Parkinson, J. S. (2002) Collaborative signaling by mixed chemoreceptor teams in *Escherichia coli*. *Proc. Natl. Acad. Sci. U.S.A.* 99, 7060–7065.
- (43) Briegel, A., Wong, M. L., Hodges, H. L., Oikonomou, C. M., Piasta, K. N., Harris, M. J., Fowler, D. J., Thompson, L. K., Falke, J. J., Kiessling, L. L., and Jensen, G. J. (2014) New insights into bacterial chemoreceptor array structure and assembly from electron cryotomography. *Biochemistry* 53, 1575–1585.
- (44) Li, G., and Weis, R. M. (2000) Covalent modification regulates ligand binding to receptor complexes in the chemosensory system of *Escherichia coli*. *Cell* 100, 357–365.
- (45) Bornhorst, J. A., and Falke, J. J. (2000) Attractant regulation of the aspartate receptor-kinase complex: Limited cooperative interactions



between receptors and effects of the receptor modification state. *Biochemistry* 39, 9486–9493.

(46) Blaser, M., Bork, P., Fraser, C., Knight, R., and Wang, J. (2013) The microbiome explored: Recent insights and future challenges. *Nat. Rev. Microbiol.* 11, 213–217.

(47) Khosravi, A., and Mazmanian, S. K. (2013) Disruption of the gut microbiome as a risk factor for microbial infections. *Curr. Opin. Microbiol.* 16, 221–227.

(48) Gegner, J. A., Graham, D. R., Roth, A. F., and Dahlquist, F. W. (1992) Assembly of an MCP receptor, CheW, and kinase CheA complex in the bacterial chemotaxis signal transduction pathway. *Cell* 70, 975–982.

(49) Chervitz, S. A., and Falke, J. J. (1995) Lock on/off disulfides identify the transmembrane signaling helix of the aspartate receptor. *J. Biol. Chem.* 270, 24043–24053.

(50) Chervitz, S. A., Lin, C. M., and Falke, J. J. (1995) Transmembrane signaling by the aspartate receptor: Engineered disulfides reveal static regions of the subunit interface. *Biochemistry* 34, 9722–9733.

(51) Borkovich, K. A., and Simon, M. I. (1991) Coupling of receptor function to phosphate-transfer reactions in bacterial chemotaxis. *Methods Enzymol.* 200, 205–214.